

# 7. The mechanism for acetylcholine receptor inhibition by $\alpha$ -neurotoxins and species-specific resistance to $\alpha$ -bungarotoxin revealed by NMR

Abraham O Samson, Tali Scherf, Miriam Eisenstein, Jordan H Chill and Jacob Anglister

---

## INTRODUCTION

---

$\alpha$ -Bungarotoxin ( $\alpha$ -BTX) is a 74 amino acid,  $\alpha$ -neurotoxin derived from the venom of the snake *Bungarus multicinctus*. It binds to the postsynaptic muscle acetylcholine receptor (AChR) with a  $K_D$  of  $10^{-11}$  M,<sup>1</sup> competitively inhibiting ACh binding, thereby preventing the depolarization of postsynaptic membranes and blocking neuromuscular transmission. Using dynamic filtering techniques, the major determinant involved in toxin binding was mapped to the segment  $^{\alpha 1}$ W184- $^{\alpha 1}$ D200 which forms a  $\beta$ -hairpin<sup>2</sup> ( $\alpha$ -BTX and AChR residues are designated by a superscript B ( $^B$ X) or  $\alpha 1$ ,  $\alpha 7$ ,  $\beta$  or  $\delta$  (i.e.  $^{\alpha 1}$ X) respectively, before the one-letter amino acid code indicating the subunit type and the position in the sequence). The dissociation constant of  $\alpha$ -BTX for a  $\alpha 1^{184-200}$  peptide is  $2.5 \times 10^{-7}$  M, two orders of magnitude higher than that for the  $\alpha 1^{185-196}$  peptide, emphasizing the importance of the N-terminal residues  $^{\alpha 1}$ P197- $^{\alpha 1}$ D200 for binding.

The structure of the entire AChR has not been solved at high resolution. Recently, Brejc et al.<sup>3</sup> determined the crystal structure of a snail ACh-binding protein (AChBP) which shares up to 30% sequence identity with AChRs. Superposition of the toxin-bound high-affinity peptide (HAP) on the analogous region of the AChBP located the binding site for  $\alpha$ -neurotoxins at the outer perimeter of the AChBP at the interface between two identical subunits.<sup>4</sup> The molecular axis of the toxin was found to be perpendicular both to the five-fold symmetry axis and to the tangent to the pentameric ring (the

molecular axis of  $\alpha$ -BTX is defined here as the long axis of the second finger). Due to the perpendicular orientation, the contact area between the toxin and the receptor is only  $760 \text{ \AA}^2$ , not accounting for the extremely high affinity between the two proteins. Moreover, the superposition used resulted in numerous Van der Waals violations between the toxin and the homopentameric AChBP that could potentially be relieved by elaborate modeling. The Van der Waals violations prevented detailed analysis of the interactions between  $\alpha$ -BTX and the heteropentameric muscle-AChR, and the interactions between the two proteins could be inferred only by analogy to the AChBP.

In the present study, we determined the solution structure of a complex between  $\alpha$ -BTX and a peptide corresponding to the segment  $^{\alpha 1}$ R182- $^{\alpha 1}$ I202 containing the entire major ligand-binding domain of *Torpedo*  $\alpha 1$ , including all residues previously found to be important for species-specific resistance to  $\alpha$ -BTX. Using our NMR structure of  $\alpha$ -BTX/ $\alpha 1^{182-202}$  complex we constructed the first homology-based model of the extracellular domain of the muscle-AChR, AChR-EC, in complex with two toxin molecules. In this model  $\alpha$ -BTX forms an angle of approximately  $35^\circ$  with the plane of the pentameric ring and a  $37^\circ$  angle with the tangent to the ring. This orientation considerably increases the contact area between AChR and  $\alpha$ -BTX. According to our model,  $>1800 \text{ \AA}^2$  of the toxin surface are buried upon receptor binding, compared with a mere  $760 \text{ \AA}^2$  in the AChBP superposition,<sup>4</sup> clearly in line with the high affinity to the receptor. The

conserved  $\alpha$ -neurotoxin residue <sup>B</sup>R36 occupies the partially buried deep pocket for ACh, thus providing a novel explanation for the mechanism of AChR inhibition by snake  $\alpha$ -neurotoxins.

---

SOLUTION STRUCTURE OF  
 $\alpha$ -BTX/ $\alpha 1^{182-202}$  COMPLEX

---

**STRUCTURE DETERMINATION OF  
 $\alpha$ -BTX/ $\alpha 1^{182-202}$  COMPLEX**

The structure determination was based on a total of 1673 NMR distance constraints. Of these constraints 522 were long range and included 375 intra-toxin, 104 peptide/toxin, and 43 intra-peptide constraints. Torsion angle constraints included 77  $\phi$ -angles and 41  $\chi_1$ -angles. Structure calculations were performed with the CNS program using the NMR-derived distance and dihedral angle constraints.<sup>5</sup> Fig. 7.1A shows the backbone superposition of 28 lowest energy structures.

The overall structure of the complex is well defined with rmsd values of 0.84 Å and 1.45 Å for the backbone and heavy atoms respectively.

**STRUCTURE OF THE BOUND  $\alpha$ -BTX**

As shown in Fig. 7.1B the overall structure of  $\alpha$ -BTX consists of three long fingers and a C-terminal tail. Finger I forms a  $\beta$ -hairpin with two anti-parallel  $\beta$ -strands consisting of residues <sup>B</sup>V2-<sup>B</sup>T6 and <sup>B</sup>I11-<sup>B</sup>T15. Finger II consists of two anti-parallel  $\beta$ -strands, <sup>B</sup>L22-<sup>B</sup>D30 and <sup>B</sup>G37-<sup>B</sup>A45. Residues <sup>B</sup>E56-<sup>B</sup>C60 of finger III form a triple-stranded anti-parallel  $\beta$ -sheet with finger II to create the central core of the toxin. These motifs are present in many  $\alpha$ -neurotoxins.<sup>6</sup>

The secondary structure of free  $\alpha$ -BTX was determined earlier.<sup>7</sup> In the  $\alpha$ -BTX complex with  $\alpha 1^{185-196}$ , residues <sup>B</sup>W28 and <sup>B</sup>V39 located at the edge of  $\beta$ -sheet of the second finger zip together upon peptide binding.<sup>8</sup> In the present study of  $\alpha$ -BTX in complex

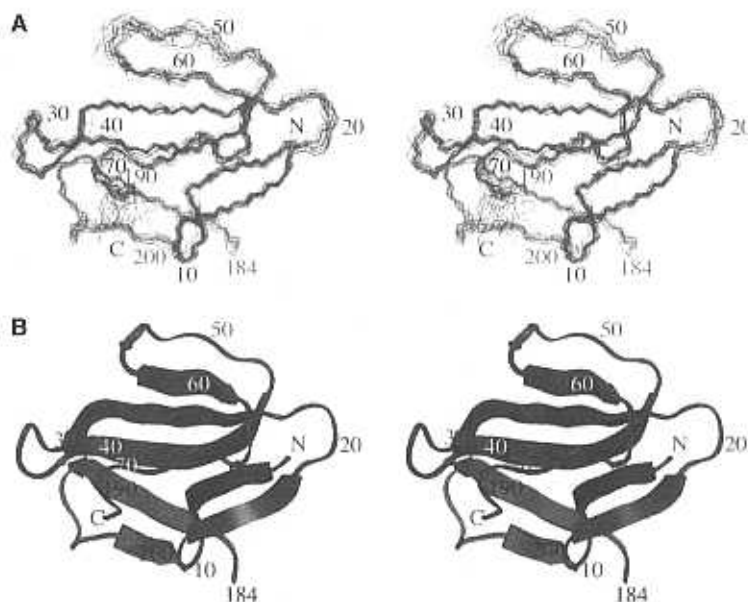


Figure 7.1 Stereo view of the  $\alpha$ -BTX/ $\alpha$ AChR<sup>182-202</sup> complex (colored in dark and light gray, respectively).

Only the peptide segment <sup>61</sup>W184-<sup>211</sup>D200, which exhibits a converged structure, is shown. N and C denote the termini of the toxin and the peptide and each tenth residue is numbered. (A) Backbone superposition of 28 lowest energy structures. (B) A ribbon diagram of the energy-minimized average structure. All figures were prepared using Insight II and MOLMOL.<sup>17</sup>

with the longer  $\alpha$ 1<sup>182-202</sup>, additional residues, namely <sup>B</sup>C29-<sup>B</sup>D30 and <sup>B</sup>G37-<sup>B</sup>K38, extend the  $\beta$ -sheet, illustrating the importance of  $\alpha$ 1<sup>182-202</sup> in stabilizing the complex.

#### STRUCTURE OF THE BOUND $\alpha$ 1<sup>182-202</sup>

As already revealed in the secondary structure determination of the bound peptide,<sup>2</sup>  $\alpha$ 1<sup>182-202</sup> adopts a  $\beta$ -hairpin conformation, consisting of two anti-parallel  $\beta$ -strands formed by residues  $\alpha$ 1<sup>H186</sup>- $\alpha$ 1<sup>T191</sup> and <sup>B</sup>Y198-<sup>B</sup>D200 (Fig. 7.2A) and a six-residue connecting loop made of  $\alpha$ 1<sup>C192</sup>- $\alpha$ 1<sup>P197</sup> (CCPDTP) rigidified by the disulfide

bond and two prolines. The first three residues of the elongated  $\beta$ -strand  $\alpha$ 1<sup>H186</sup>- $\alpha$ 1<sup>T191</sup> interact with the second  $\beta$ -strand of  $\alpha$ 1<sup>182-202</sup>,  $\alpha$ 1<sup>Y198</sup>- $\alpha$ 1<sup>D200</sup>, thus closing the  $\beta$ -hairpin, while the last three residues of the first strand, namely  $\alpha$ 1<sup>Y189</sup>- $\alpha$ 1<sup>T191</sup>, associate with the toxin residues <sup>B</sup>K38-<sup>B</sup>V40, to form an intermolecular  $\beta$ -sheet (Fig. 7.2A). The upper face of the  $\beta$ -hairpin is formed by the side-chains of residues  $\alpha$ 1<sup>K185</sup>,  $\alpha$ 1<sup>W187</sup>,  $\alpha$ 1<sup>Y189</sup>,  $\alpha$ 1<sup>P194</sup>,  $\alpha$ 1<sup>P197</sup>, and  $\alpha$ 1<sup>L199</sup>, while the lower face is formed by the side-chains of  $\alpha$ 1<sup>H186</sup>,  $\alpha$ 1<sup>V188</sup>,  $\alpha$ 1<sup>Y190</sup>,  $\alpha$ 1<sup>C192</sup>,  $\alpha$ 1<sup>C193</sup>,  $\alpha$ 1<sup>Y198</sup>, and  $\alpha$ 1<sup>D200</sup>, thus stabilizing the  $\beta$ -hairpin conformation through mostly hydrophobic interaction (Fig. 7.2A).

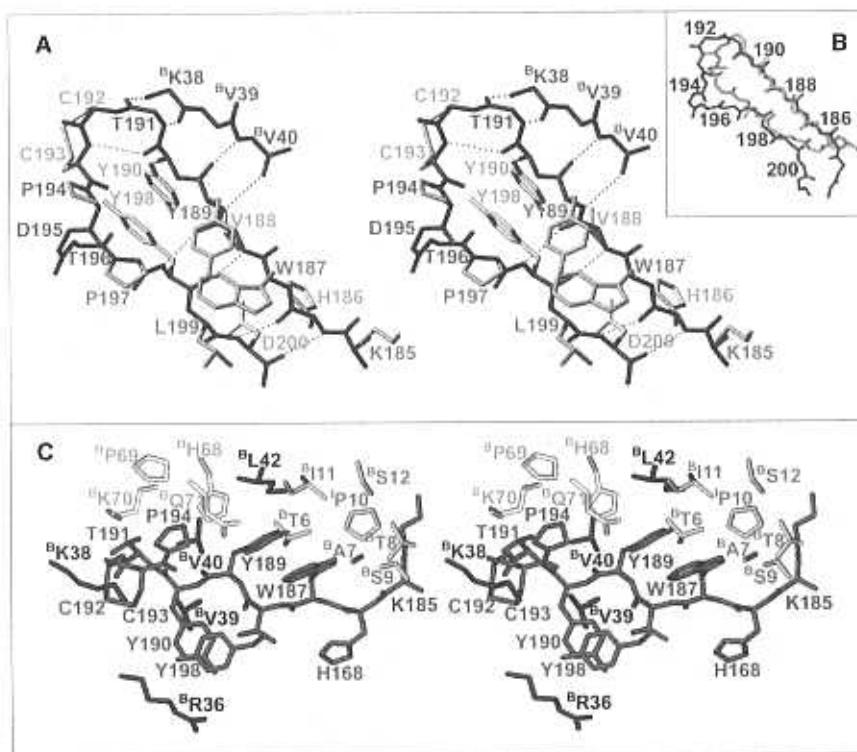


Figure 7.2 The structure and interactions of the  $\alpha$ -BTX-bound  $\alpha$ 1<sup>182-202</sup>.

(A) Stereo representation of the hydrogen bonding and intramolecular side-chain interactions of the bound  $\alpha$ 1<sup>182-202</sup>. Intramolecular hydrogen bonds within the peptide, and intermolecular hydrogen bonds with <sup>B</sup>K38-<sup>B</sup>V40 are in dotted lines. (B) Superposition of the  $\alpha$ 1<sup>H186</sup>- $\alpha$ 1<sup>D200</sup> segment and the corresponding segment of AChBP (N181-D194). The backbone atoms of  $\alpha$ 1<sup>182-202</sup> (light gray) and the corresponding AChBP segment (dark gray) are shown. (C) A stereo representation of side-chain interactions of  $\alpha$ 1<sup>182-202</sup> with  $\alpha$ -BTX. The peptide interacts with the first finger, second finger, and C-terminus of  $\alpha$ -BTX residues denoted by a superscript B.

The corresponding region of AChBP (KKNSV-TYSCPEAYEDV, residues 179–194) was found to adopt a  $\beta$ -hairpin conformation, in which Ser<sup>186</sup>-Cys<sup>187</sup> form a turn.<sup>3</sup> Backbone superposition of the  $\alpha$ -BTX bound AChR segments  $\alpha^1$ K185– $\alpha^1$ Y190 and  $\alpha^1$ Y198– $\alpha^1$ L199 over that of the corresponding AChBP region resulted in an rmsd of 1.4 Å (Fig. 7.2B), a deviation originating mostly from the one-residue insertion  $\alpha^1$ P194 in the AChR sequence. The two prolines ( $\alpha^1$ P194,  $\alpha^1$ P197) of  $\alpha^1$ 182–202 break the  $\beta$ -structure and produce a  $\beta$ -bulge consisting of the segment  $\alpha^1$ P194– $\alpha^1$ P197. The second  $\beta$ -strand in AChBP extends beyond its three-residue counterpart in  $\alpha^1$ 182–202 ( $\alpha^1$ Y198– $\alpha^1$ D200).

#### BINDING INTERACTIONS OF $\alpha^1$ 182–202 AND THE TOXIN

Surrounded by the toxin,  $\alpha^1$ 182–202 fits snugly into the  $\alpha$ -BTX binding site. As shown in Fig. 7.2C, 12  $\alpha^1$ 182–202 residues interact with 19 toxin residues. The side-chains of  $\alpha^1$ K185,  $\alpha^1$ W187, and  $\alpha^1$ Y189 interact through mostly hydrophobic interaction with residues <sup>B</sup>T6–<sup>B</sup>S12 of the first finger of  $\alpha$ -BTX. Peptide residues  $\alpha^1$ Y189– $\alpha^1$ T191 interact with residues <sup>B</sup>K38–<sup>B</sup>V40 of the toxin  $\beta$ -sheet core through an intermolecular  $\beta$ -sheet involving four hydrogen bonds (Fig. 7.2A). Hydrophobic interactions between  $\alpha^1$ Y189 and <sup>B</sup>V40 on the upper side of the  $\beta$ -hairpin and between  $\alpha^1$ Y190 and <sup>B</sup>V39 on the lower side of the  $\beta$ -hairpin help to stabilize the intermolecular  $\beta$ -sheet. The side-chains of tyrosines  $\alpha^1$ Y190 and  $\alpha^1$ Y198 on the lower side of the  $\beta$ -hairpin interact with <sup>B</sup>R36 of the toxin's second finger, a highly conserved toxin residue found to be important for toxin binding to AChR (see below). Finally, residues  $\alpha^1$ Y189,  $\alpha^1$ T191,  $\alpha^1$ C192, and  $\alpha^1$ P194 interact through mostly hydrophobic interaction with residues <sup>B</sup>H68–<sup>B</sup>Q71 at the C-terminus of the toxin (Fig. 7.2C). Residues  $\alpha^1$ K185,  $\alpha^1$ W187,  $\alpha^1$ Y189,  $\alpha^1$ Y190,  $\alpha^1$ T191,  $\alpha^1$ C192, and  $\alpha^1$ P194 are the strongest contributors to the contact surface between  $\alpha^1$ 182–202 and the toxin.

#### NMR-DERIVED MODEL OF THE AChR-EC/ $\alpha$ -BTX COMPLEX

##### MODELING OF THE AChR-EC/ $\alpha$ -BTX COMPLEX

The AChBP sequence was aligned with those of various AChR subunits using the Clustal W program.<sup>9</sup> The sequence identity between AChBP and each AChR-EC subunit is only 19–24%.<sup>3</sup> Nevertheless, the sequence alignment of the AChBP monomer and each of the AChR-EC subunits showed a good fit with almost no gaps over the entire sequence (Fig. 7.3A). The highest similarity was found in the secondary structure elements. The cysteine pair  $\alpha^1$ C128 and  $\alpha^1$ C142 is conserved in all AChR-EC subunits, while the vicinal  $\alpha^1$ C192 and  $\alpha^1$ C193 pair is conserved in  $\alpha$ -subunits only.

The AChBP subunit consisting of 210 amino acids served as a template for our model. Each subunit of the AChR model was therefore delimited to this size and the following segments,  $\alpha$ 1(2–211),  $\delta$ (2–225),  $\gamma$ (2–219), and  $\beta$ (2–217), corresponding to the 210-residue subunit of AChBP were modeled. Inserts in the  $\delta$ -,  $\gamma$ -, and  $\beta$ -sequences increase the length of the respective subunit. Using the homology module of the Accelrys package, the residues in the structurally conserved regions of AChBP were replaced by those of AChR-EC, resulting in minor side-chain collisions, which were repaired by assigning suitable rotamers conformation. Random loops were generated for the segments connecting structurally conserved regions, producing few molecular Van der Waals violations, which were alleviated by manually assigning alternative rotamers to the side-chains of colliding residues.

To dock two  $\alpha$ -BTX molecules into the AChR model,  $\alpha^1$ 182–202 residues 185–190 and 198–199 from the NMR structure of the  $\alpha$ -BTX/ $\alpha^1$ 182–202 complex were superimposed on the corresponding residues in the AChR model, resulting in an rmsd of 1.4 Å. Residues  $\alpha^1$ 185– $\alpha^1$ 200 of the  $\alpha^1$  model were assigned with the cartesian coordinates of the corresponding  $\alpha^1$ 182–202 segment of the complex



## THE ION CHANNEL OF AChR

AChBP is a soluble protein found in the synaptic cleft, where it modulates synaptic transmission. It consists of five identical subunits arranged as a doughnut to form a central pore. This protein is not a cation channel and therefore does not require a negatively charged duct along its five-fold axis. Indeed, the electrostatic potential map of AChBP presents a slightly positively charged cavity on one side and a slightly negative cavity on the other side. On the other hand, the heteropentameric AChR forms a strongly negative duct, which measures 1–1.5 nm in radius, and 5 nm in height. Several residues lining the inner perimeter of the AChR channel duct are different from those of the AChBP. Uncharged amino acids of the AChBP are mutated to negatively charged ones (i.e. S79 to  $^{\alpha 1}D/\gamma^{\delta}E$ , S80 to  $^{\alpha 1}\beta D$ , S93 to  $^{\alpha 1}\beta/\gamma^{\delta}D$ ) and positively charged to negative or neutral residues (i.e. H69 to  $^{\alpha 1}D/\gamma^{\delta}E/\beta A$ , K94 to  $^{\alpha 1}D/\gamma^{\delta}Q/\beta S$ ).

## RELATIVE TOXIN ORIENTATION ON AChR

$\alpha$ -BTX forms an angle of approximately  $35^{\circ}$  with the plane of the pentameric ring of AChR and a  $37^{\circ}$  angle with the tangent to the ring (Fig. 7.3B and C). In contrast, the superimposed model of Harel et al<sup>1</sup> located  $\alpha$ -BTX in the plane of the pentameric ring and perpendicular to the tangent to the AChBP

ring. The different angular orientation of  $\alpha$ -BTX in the AChR model dramatically increases its contact area with the receptor by a factor of  $\sim 2.5$  (see below).

BINDING INTERFACE OF  $\alpha$ -BTX AND AChR

Almost all the interactions of the  $\alpha 1$ -subunit with the toxin arise from residues  $^{\alpha 1}K185$ – $^{\alpha 1}I199$ , the only exception being the interaction of  $^{\alpha 1}W149$  with  $^{\beta}R36$ . The first finger of the toxin interacts with the  $\alpha 1$ -subunit only. The long second finger of  $\alpha$ -BTX penetrates deeply into the interface between the  $\alpha 1\gamma$  and the  $\alpha 1\delta$  subunits and residues  $^{\beta}K26$ – $^{\beta}E41$  ( $^{\beta}R36$  included) interact extensively with both subunits but mostly with the  $\gamma$ - and  $\delta$ -subunits. The third finger interacts with the  $\gamma$ - and  $\delta$ -subunits and the C-terminus of the toxin interacts only with the  $\alpha 1$ -subunit.

 $^{\beta}R36$  OCCUPIES ACETYLCHOLINE-BINDING POCKET

The most striking feature of the NMR-derived model of the AChR/ $\alpha$ -BTX complex is the occupation of the ACh binding site by  $^{\beta}R36$  (Fig. 7.4A and B).  $^{\beta}R36$  mimics ACh (Fig. 7.4C) thus occluding neurotransmitter binding. The majority of the receptor residues interacting with  $^{\beta}R36$  are from

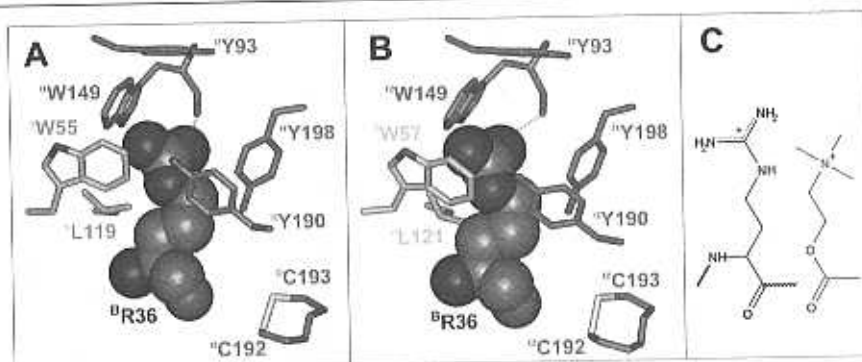


Figure 7.4 Interactions of  $\alpha$ -BTX with AChR-EC in the NMR-derived model.

(A) Interactions of  $\alpha$ -BTX  $^{\beta}R36$  in the ACh binding pocket of AChR at the interface between the  $\alpha 1$ - and  $\gamma$ -subunits and (B) at the interface between the  $\alpha 1$ - and  $\delta$ -subunits. (C) Structural comparison between ACh (right) and the arginine residue (left).

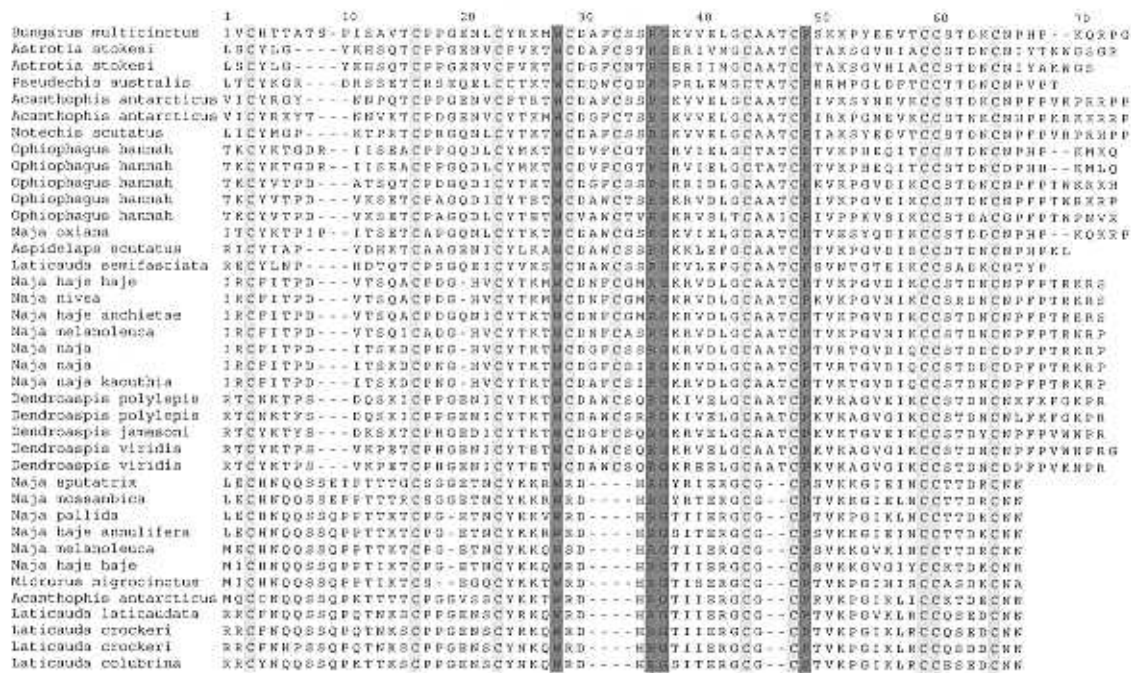


Figure 7.5 Sequence alignment of various  $\alpha$ -neurotoxins.

The invariant cysteine residues (light gray), and non-cysteine residues (dark gray) are highlighted.

the  $\alpha$ 1-subunit. The positively charged guanidinium group of <sup>B</sup>R36 forms cation- $\pi$  interactions with  <sup>$\alpha$ 1</sup>W149,  <sup>$\delta$</sup> W57 ( <sup>$\gamma$</sup> W55 in the  $\gamma$ -subunit), and possibly with  <sup>$\alpha$ 1</sup>Y93. In addition a hydrogen bond is formed between the guanido group of <sup>B</sup>R36 and the carbonyl oxygen of  <sup>$\alpha$ 1</sup>W149.  <sup>$\alpha$ 1</sup>Y190,  <sup>$\alpha$ 1</sup>Y198, and  <sup>$\delta$</sup> L121 ( <sup>$\gamma$</sup> L119 in the  $\gamma$ -subunit) interact with the methylenes of the <sup>B</sup>R36 side-chain.  <sup>$\alpha$ 1</sup>C192 and  <sup>$\alpha$ 1</sup>C193 are close to the carbonyl group of <sup>B</sup>R36 and the methylene group of <sup>B</sup>G37. Notably, the orientation of <sup>B</sup>R36 in the AChR/ $\alpha$ -BTX model is dictated by the interactions with  <sup>$\alpha$ 1</sup>Y190 and  <sup>$\alpha$ 1</sup>Y198 as observed by NMR and was not changed during the modeling process.

The NMR-derived model of the  $\alpha$ -BTX/AChR complex is in remarkable agreement with pairwise interactions between AChR and the short  $\alpha$ -neurotoxin *Naja mossambica mossambica I* (*Nnm1*) revealed by double mutant cycle experiments.<sup>10,11</sup> The *Nnm1* R33 (homologous to <sup>B</sup>R36, see Fig. 7.5)

was found to interact with  <sup>$\gamma$</sup> L119 and  <sup>$\gamma$</sup> W55, and a cation- $\pi$  interaction between  <sup>$\gamma$</sup> W55 and the *Nnm1* R33 was suggested.<sup>11</sup> In addition, *Nnm1* R33 was found to be coupled to  <sup>$\alpha$ 1</sup>W149,  <sup>$\alpha$ 1</sup>V188,  <sup>$\alpha$ 1</sup>Y190,  <sup>$\alpha$ 1</sup>Y198, and  <sup>$\alpha$ 1</sup>D200 of the  $\alpha$ 1-subunit. It was thus suggested that *Nnm1* R33 is inserted between the  $\alpha$ 1- and  $\gamma$ -subunits and anchors the  $\alpha$ -toxin to the surfaces of both subunits,<sup>10</sup> exactly as observed for <sup>B</sup>R36 in our NMR-derived model of  $\alpha$ -BTX complex with AChR (see Fig. 7.4A and B).

**<sup>B</sup>R36 IS INVARIANT IN SNAKE  $\alpha$ -NEUROTOXINS**

Sequence alignment of several long and short  $\alpha$ -neurotoxins displayed a high sequence identity (35–65%) as well as five invariant cystine bridges (Fig. 7.5). The alignment revealed that the arginine at the tip of the second finger, <sup>B</sup>R36, and <sup>B</sup>G37 are invariant (Fig. 7.5). As mentioned earlier, <sup>B</sup>R36

occupies the ACh-binding site on the receptor, while the small and flexible <sup>B</sup>G37 enables optimal fit of <sup>B</sup>R36 in the ACh-binding pocket. These findings are in excellent agreement with mutagenesis results that show that a mutation of R33 of *Nnml* (homologous to <sup>B</sup>R36, see Fig. 7.5) results in four orders of magnitude decrease in the affinity of the toxin to AChR.<sup>11</sup> In addition to <sup>B</sup>R36 and <sup>B</sup>G37, residues <sup>B</sup>W28 and <sup>B</sup>P49 were the only invariant residues excluding the cysteines. Remarkably, <sup>B</sup>W28 interacts extensively with the  $\gamma$ - and  $\delta$ -subunits.<sup>12</sup>

#### NMR STRUCTURE OF THE $\alpha$ -BTX COMPLEXED WITH $\alpha$ 1<sup>182-202</sup> ACCOUNTS FOR SPECIES-SPECIFIC SUSCEPTIBILITY TO THE TOXIN

Snake neurotoxins have evolved to paralyze the snake's prey by inactivating muscle AChR and, therefore, both long and short  $\alpha$ -neurotoxins exhibit high affinity to muscle AChR and its  $\alpha$ 1-subunit. In Fig. 7.6, sequences of the  $\alpha$ 1 of various species are presented together with their relative binding affinity to  $\alpha$ -BTX.<sup>13-15</sup> The natural prey of the snake *Bungarus multicinctus* are frogs and chicks, and it is therefore not surprising that  $\alpha$ -BTX binds lethally and with the highest affinity to their  $\alpha$ 1. The *Torpedo californica*  $\alpha$ 1 sequence is similar to that of frogs, and therefore, exhibits similar affinities.<sup>13</sup> On the other hand, snakes themselves and their predators such as the mongoose are naturally resistant to snake venom in general, and  $\alpha$ -BTX in particular.<sup>16</sup> Other species such as humans and hedgehogs, the latter being closely related to the mongoose, exhibit reduced sensitivity to  $\alpha$ -BTX poisoning.<sup>15</sup> Understanding the influence of a mutation on the actual binding is a powerful tool in relating  $\alpha$ 1 structure to its function.

The  $\beta$ -hairpin  $\alpha$ 1K185- $\alpha$ 1D200 is the major  $\alpha$ 1-subunit determinant involved in both ACh and snake toxin binding, protruding out of the  $\alpha$ 1-subunit as a long tongue. While the upper and lower face of the  $\beta$ -hairpin and the backbone of the N-terminal  $\beta$ -strand ( $\alpha$ 1Y189- $\alpha$ 1T191) are involved in toxin binding (see Fig. 7.2), only the lower face is involved directly in ACh binding. Resistance to

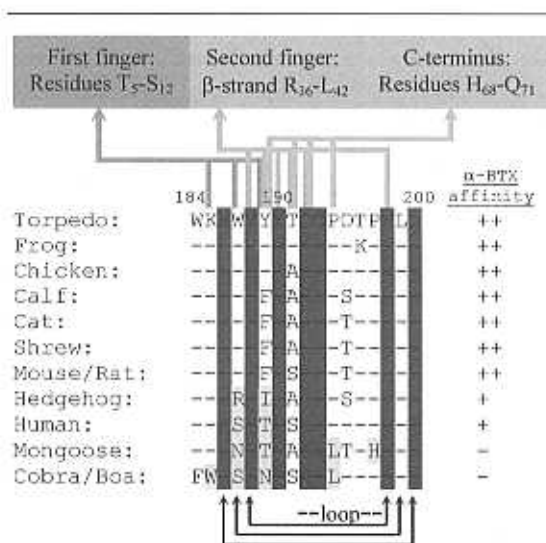


Figure 7.6 Sequence comparison of  $\alpha$ 1 of different species showing the segment 184-200.

Affinities to  $\alpha$ -BTX are obtained from Ohana and Gershoni,<sup>13</sup> Conti-Tronconi et al.,<sup>14</sup> and Barchan et al.<sup>15</sup>  $\alpha$ 1 residues interacting with  $\alpha$ -BTX are marked with gray arrows and Residues involved in the intramolecular  $\beta$ -strand/ $\beta$ -strand interactions are marked with black arrows. Conserved  $\alpha$ 1 residues are highlighted in dark gray, and natural mutations leading to a decrease or abolition of  $\alpha$ -BTX affinity are highlighted in light gray.

snake toxins can therefore be obtained by mutating residues with side-chains pointing to the upper face while conserving those with side-chains pointing downwards and that are crucial for ACh binding. Fig. 7.6 indicates that mutations of residues  $\alpha$ 1K185,  $\alpha$ 1W187,  $\alpha$ 1Y189,  $\alpha$ 1P194, and  $\alpha$ 1P197 lead to a decrease or loss of toxin-binding capability. In snakes, resistance to  $\alpha$ -neurotoxins is conferred by the  $\alpha$ 1K185W,  $\alpha$ 1W187S,  $\alpha$ 1Y189N, and  $\alpha$ 1P194L mutations while in mongoose resistance is obtained by  $\alpha$ 1W187N (putatively N-glycosylated),  $\alpha$ 1Y189T,  $\alpha$ 1P194L, and  $\alpha$ 1P197H mutations.<sup>15</sup> Our structure indicates that the side-chains of residues  $\alpha$ 1K185,  $\alpha$ 1W187,  $\alpha$ 1Y189, and  $\alpha$ 1P194 point to the upper side of the  $\beta$ -hairpin and interact extensively with  $\alpha$ -BTX. The aforementioned mutations obviate the favorable interactions with the toxin and abolish its binding. Fig. 7.6 also indicates that mutations of residues  $\alpha$ 1D195 and  $\alpha$ 1T196 do not significantly alter the AChR affinity to the toxin. In

susceptible species such as frogs,  $^{\alpha 1}$ T196 is replaced by a lysine, whereas in cats  $^{\alpha 1}$ D195 is replaced by threonine. Interestingly,  $T_1$  relaxation time in the rotating-frame ( $T_{1\rho}$ ) and rmsd values of residues  $^{\alpha 1}$ D195 and  $^{\alpha 1}$ T196 suggest that they are more flexible than other residues within the binding determinant (Samson et al, unpublished results). Our findings suggest that these residues are solvent-exposed in  $\alpha 1^{182-202}$  and do not contribute to  $\alpha$ -BTX binding. Finally, Fig. 7.6 shows that residues  $^{\alpha 1}$ H186,  $^{\alpha 1}$ V188,  $^{\alpha 1}$ Y190,  $^{\alpha 1}$ C192,  $^{\alpha 1}$ C193,  $^{\alpha 1}$ Y198, and  $^{\alpha 1}$ D200, which form the lower face of the  $\beta$ -hairpin, are conserved. Four of these residues, namely,  $^{\alpha 1}$ Y190,  $^{\alpha 1}$ C192,  $^{\alpha 1}$ C193,  $^{\alpha 1}$ Y198, form the binding site for ACh and interact with  $^B$ R36, which mimics ACh.

## CONCLUSION

The structure of the major acetylcholine receptor determinant in complex with  $\alpha$ -BTX was solved using NMR spectroscopy. The AChR-peptide folds into a  $\beta$ -hairpin which associates with the  $\alpha$ -BTX central  $\beta$ -sheet through hydrogen bonds and hydrophobic interactions. One face of the peptide  $\beta$ -hairpin, that is exposed to  $\alpha$ -BTX, presents variable amino acids which confer toxin resistance to species such as mongoose and cobra. Residues on the other face of the  $\beta$ -hairpin are highly conserved in different animal species, because they are involved in acetylcholine binding. Based on this NMR structure, and on that of the AChBP, we constructed a model of the toxin-bound AChR. Remarkably,  $^B$ R36 at the second fingertip of the toxin occupies the receptor-binding site, thereby occluding ACh binding and preventing channel opening. This arginine is invariant in  $\alpha$ -neurotoxins originating from different snake species. The channel duct formed in the center of the AChR pentameric ring is negatively charged to assist cation flux. The toxin molecules form an angle of  $35^\circ$  with the tangent of this ring, considerably increasing the contact area. This study,<sup>12</sup> provides a new explanation for the AChR inhibition

by snake  $\alpha$ -neurotoxins and sheds light on the ligand-binding pocket and channel duct at atomic resolution.

## ACKNOWLEDGMENTS

We thank Mrs Aviva Kapitkovski and Mr Yehezkiel Haik for synthesizing and purifying the AChR-peptides.

## REFERENCES

1. Stroud RM, McCarthy MP, Shuster M. Nicotinic acetylcholine receptor superfamily of ligand-gated ion channels. *Biochemistry* 1990; **29**: 11009–23.
2. Samson AO, Chill JH, Rodriguez E, Scherf T, Anglister J. NMR mapping and secondary structure determination of the major acetylcholine receptor  $\alpha$ -subunit determinant interacting with  $\alpha$ -bungarotoxin. *Biochemistry* 2001; **40**:5464–73.
3. Brejc K, van Dijk WJ, Klaassen RV et al. Crystal structure of an ACh-binding protein reveals the ligand-binding domain of nicotinic receptors. *Nature* 2001; **411**:269–76.
4. Harel M, Kasher R, Nicolas A et al. The binding site of acetylcholine receptor as visualized in the X-ray structure of a complex between  $\alpha$ -bungarotoxin and a mimotope peptide. *Neuron* 2001; **32**:265–75.
5. Brünger AT, Adams PD, Clore GM et al. Crystallography & NMR system: a new software suite for macromolecular structure determination. *Acta Crystallogr D Biol Crystallogr* 1998; **54**:905–21.
6. Tselin V. Snake venom  $\alpha$ -neurotoxins and other 'three-finger' proteins. *Eur J Biochem* 1999; **264**:281–6.
7. Basus VI, Billeter M, Love RA, Stroud RM, Kurtz ID. Structural studies of  $\alpha$ -bungarotoxin. I. Sequence-specific  $^1$ H NMR resonance assignments. *Biochemistry* 1988; **27**:2763–71.
8. Basus VI, Song G, Hawrot E. NMR solution structure of an  $\alpha$ -bungarotoxin/nicotinic receptor peptide complex. *Biochemistry* 1993; **32**:12290–8.
9. Thompson JD, Higgins DG, Gibson TJ. CLUSTAL W: improving the sensitivity of progressive multiple sequence alignment through sequence weighting, positions-specific gap penalties and weight matrix choice. *Nucleic Acids Res* 1994; **22**:4673–80.
10. Malany S, Osaka H, Sine SM, Taylor P. Orientation of  $\alpha$ -neurotoxin at the subunit interfaces of the nicotinic acetylcholine receptor. *Biochemistry* 2000; **39**:15388–98.
11. Osaka H, Malany S, Molles BE, Sine SM, Taylor P. Pairwise electrostatic interactions between  $\alpha$ -neurotoxins and  $\gamma$ ,  $\delta$ , and  $\epsilon$  subunits of the nicotinic acetylcholine receptor. *J Biol Chem* 2000; **275**:5478–84.
12. Samson AO, Scherf T, Eisenstein M, Chill JH, Anglister J. The mechanism for acetylcholine receptor inhibition by  $\alpha$ -neurotoxins and species specific resistance to  $\alpha$ -bungarotoxin revealed by NMR. *Neuron* 2002; **35**:319–32.
13. Ohana B, Gershoni JM. Comparison of the toxin binding sites of the nicotinic acetylcholine receptor from *Drosophila* to human. *Biochemistry* 1990; **29**:6409–15.

14. Corti-Tronconi BM, Diethelm BM, Wu XD et al.  $\alpha$ -Bungarotoxin and the competing antibody WF6 interact with different amino acids within the same cholinergic subsite. *Biochemistry* 1991; **30**:2575-84.
15. Barchan D, Ovadia M, Kochva E, Fuchs S. The binding site of the nicotinic acetylcholine receptor in animal species resistant to alpha-bungarotoxin. *Biochemistry* 1995; **34**:9172-6.
16. Barchan D, Kachalsky S, Neumann D et al. How the mongoose can fight the snake: the binding site of the mongoose acetylcholine receptor. *Proc Natl Acad Sci U S A* 1992; **89**:7717-21.
17. Koradi R, Billeter M, Wüthrich K. MOLMOL: a program for display and analysis of macromolecular structures. *J Mol Graph* 1996; **14**(1):29-32, 51-5.